Operations Research Forum (2024) 5:71
https://doi.org/10.1007/s43069-024-00347-3

RESEARCH

A Time-Dependent Subgraph-Capacity Model for Multiple Shortest Paths and Application to CO_2/Contrail-Safe Aircraft Trajectories

Céline Demouge[1] · Marcel Mongeau[1] · Nicolas Couellan[1,2] · Daniel Delahaye[1]

Received: 26 May 2023 / Accepted: 4 July 2024

Abstract
This paper proposes a study motivated by the problem of minimizing the environmental impact of air transport considering the complete air network, thereby several aircraft. Both CO_2 and non-CO_2 effects are taken into account to calculate this impact. The proposed methodology takes a network point of view in which airspace capacities evolve as well as the traffic itself over time. Finding the shortest path with numerous constraints and various cost functions is a common problem in operations research. This study deals with the special case of multiple shortest paths with capacity constraints on a time-dependent subgraph. Multiple shortest paths are understood as one shortest path per vehicle considered. The static special case is modeled as a mixed integer linear program so that it can be efficiently solved by standard off-the-shelf optimization solvers. The time-dependent nature of the problem is then modeled via a sliding-window approach. Encouraging numerical results on the contrail-avoidance application show that the environmental impact can be significantly reduced while maintaining safety by satisfying the airspace capacity constraints.

Keywords Subgraph constrained time-dependent shortest-path problem · Contrails · Air transportation · Mixed integer linear programming

✉ Céline Demouge
celine.demouge@enac.fr

Marcel Mongeau
mongeau@recherche.enac.fr

Nicolas Couellan
nicolas.couellan@recherche.enac.fr

Daniel Delahaye
delahaye@recherche.enac.fr

1 ENAC, Université de Toulouse, 7 Avenue Edouard Belin, Toulouse 31400, France

2 Institut Mathématiques de Toulouse, UMR 5219, Université de Toulouse, CNRS, UPS, Toulouse Cedex 9, 31062, France

Published online: 08 August 2024

1 Introduction

Transportation, and in particular air transportation, offers an important source of operations research problems, such as the shortest path under constraints. Motivated by the question of more eco-responsible transport and in a sustainable development approach, these problems generally focus on the minimization of environmental costs. In particular, for air transport, driven by a global will of the sector, the issues of green operations are gaining importance.

The air transportation environmental impact is not solely due to CO_2 effects. The non-CO_2 effects involve other greenhouse effect gases such as nitrogen oxide (NO_x) or other more complex phenomena like condensation trails (named *contrails* hereafter). Contrails form white trails at the back of the aircraft engines under certain conditions of humidity and temperature. They can disappear very quickly or on the contrary persist and turn into clouds, called cirrus [1]. These can cause a parasol effect, usually during the day, preventing the solar rays from reaching the Earth. On the contrary, they can also create a greenhouse effect, by reflecting the rays emitted by the Earth. In total, despite the important uncertainties that remain, contrails have a negative effect on the climate [2].

Avoiding contrails, therefore, requires aircraft to avoid certain areas that are favorable to their formation. These areas are zones where humidity is above a given threshold value, and the temperature under another given threshold value. See Appendix B for more details about the computation of contrail areas. Avoiding these areas is, therefore, important in order to minimize the total environmental impact. However, if this costs too much in terms of CO_2, a contrail area should not be avoided. Areas that are favorable to contrails should, therefore, be viewed as soft obstacles, and the expression "contrail avoidance" used in the sequel does not refer to a hard constraint. Different metrics to compare the effect of CO_2 and the contrail impact are proposed in the literature. This study focuses on the Global Warming Potential metric [3], which corresponds to a penalty for flying through contrail areas. It is described later in this paper (Section 4.2). Remark that contrails are not to be avoided at the expense of flight safety. This study proposes to plan flight trajectories a few hours before take-offs or in quasi-real time, where information is fixed for a given amount of time, and enriched with updated information at the end of the time period. Contrail data are too uncertain several hours before the flight, the strategic phase is then not studied here. In contrast, weather data are not continuously updated, but at a given time frequency (for instance every 30 min or hours), so a real-time approach is not appropriate.

At this scale, ensuring safety means satisfying airspace capacity constraints. Indeed, the airspace is divided into sectors under the responsibility of one or several air traffic controllers. Thus, by limiting the number of aircraft per sector per time period, it is understood that the air traffic controllers' workload will be acceptable to ensure safety. On a shorter time scale, a few minutes before arriving in an airspace sector for example, the air traffic controllers ensure safety by enforcing vertical and horizontal separations between aircraft.

To satisfy airspace capacity constraints, two approaches are possible: an airline-centered or a network-centered approach. On the one hand, flight operators propose

several flight plans and the network manager[1] looks for a valid and best potential combination. On the other hand, the computations are done directly by the network manager, assimilated in the sequel to the air traffic control. This network-centered approach allows one to reach an optimum, to avoid more cases without a solution satisfying the capacity constraints and to evaluate the consequences of politics to avoid the negative impact of contrails. This approach is the one chosen in this paper.

The considered problem is close to the classical operations research issue of finding shortest paths, which includes several types of problems. A first example is the well-known standard shortest-path problems which can be solved by efficient polynomial-time algorithms. There are several extensions of this classical problem, for instance, the time-dependent shortest-path problem with dynamic costs and constraints. Variants involving constraints are NP-hard problems even when dealing with a single vehicle. Other problems deal with several vehicles simultaneously. The problem under study is at the intersection of these mentioned problems: one seeks paths for several vehicles, under constraints, and with dynamic costs and constraints.

The main contribution of this paper is the proposition of a network approach for contrail avoidance. This low environmental-impact aircraft trajectory application comes with a realistic illustrative instance, that is made publically available, and preliminary numerical experiments that show that contrails can be mitigated at the network scale. First, an optimization model first is proposed for the static case. It computes *simultaneously* (not sequentially) a path for each vehicle considered that satisfies capacity constraints on subgraphs. A sliding-window methodology is then proposed to address time-dependent costs and constraints. This heuristic enables the problem to be solved a few hours before flight departure, or in quasi-real-time, taking into account information updated as time passes and the time window changes.

This paper proposes first in Section 2 a literature review of individual route optimization for contrail avoidance and route optimization for several vehicles. Then, it presents in Section 3 an optimization model for the static case and its extension to the time-dependent problem. The application to the contrail-avoidance aircraft trajectory problem is addressed in Section 4. Promising numerical experiments are shown and discussed in Section 5 through a sensitivity analysis of the different parameters involved. Section 6 presents general conclusions and perspectives. Appendix A gives the time-discretized optimization model, and Appendix B details how the application input data are computed.

2 Previous Related Works

This section presents previous related works by focusing first, in Section 2.1, on individual route optimization for contrail avoidance. Then, in Section 2.2, different works done on assigning routes for several vehicles are presented.

[1] National or international entity that aims to ensure the best possible use of the airspace according to its capacities by adapting the traffic. In Europe, the network manager is Eurocontrol. In the United States, the equivalent is the Air Traffic Control System Command Center (ATCSCC).

2.1 Individual Route Optimization for Contrail Avoidance

In recent years, driven by various initiatives, the issue of green aviation has become more prominent in the literature. For instance, finding trajectories with the least possible CO_2 emissions is a topic well represented in the literature in particular by proposing studies calculating the optimal wind trajectories (see for instance [4–6]). In addition, non-CO_2 effects are a particularly important topic. Several methods taking different points of view and with different resolution strategies have been developed. In the sequel, only one non-CO_2 effect is taken into account: contrails.

To solve the problem in the most general case, optimal control methods have been implemented. Since the constraints related to the mechanics of flight are enforced, the computed trajectory is flyable in the free space. The methods chosen differ according to the dimension of the instance addressed, the objective function considered, and the number of aircraft involved. In [7], the problem is solved in 2D, thanks to optimal control by minimizing an objective function that takes into account contrail avoidance, fuel, and flight time. It has been used on one-aircraft instances but also for trajectories between 12 city pairs. Hartjes et al. [8] solve the problem in 3D for a single aircraft, also by minimizing fuel, time, and time in contrail areas. Some other papers present methods taking into account time, such as [9].

Other studies rely on metaheuristics to solve the problem. For instance, Yin et al. [10] use genetic algorithms to compute transatlantic flight trajectory to mitigate the impact of contrails. Methods based on graphs are also used, like A* in [11] or Dijkstra's algorithm [12].

Finally, other methodologies rely on mixed integer linear program [13] or on mixed integer quadratic programming [14] formulations.

Simorgh et al. remark in [15] that Air Traffic Management (ATM) considerations are less often taken into account when multiple aircraft are considered, although the impact on airspace capacity and controller workload is certain. Indeed, a risk is to empty the spaces favorable to contrails by strongly congesting adjacent airspaces. Addressing problems that aim at avoiding such situations is one of the main contributions of this paper.

2.2 Assigning Routes for Several Vehicles

Finding the shortest path is a common problem in operations research. The literature presents various ways to solve such problems. The graph version of the problem can be addressed by integer linear programming [16], or other efficient algorithms such as Dijkstra's algorithm [17], A* [18] or Bellman's algorithm [19] (dynamic programming). In some cases, optimal control techniques [20] can be used, especially if the path is to be computed in a continuous space and not on a graph. Variants of the shortest path problem are subject to constraints that typically involve an upper limit on a function of the arcs. For instance, the goal can be to minimize the distance traveled by a vehicle with an upper bound on the travel time. This type of problem is usually expressed for one vehicle, for one path. It is an NP-hard problem for which some efficient methods have been developed [21–24].

Some other problems compute several shortest paths, i.e., several vehicles are considered via a global criterion to be minimized. This is the case for the *traffic assignment problem* (TAP) which aims at reaching an equilibrium for the vehicles or for the whole system. The type of chosen equilibrium determines the objective function to be minimized. An example is the *Wardrop user and system equilibrium* [25, 26]. The problem is subject to flow conservation constraints and capacity constraints on arcs and, in the case of *system equilibrium*, it minimizes the average journey cost. This problem considers cooperation and possibly a decentralized management of the traffic. On the other hand, the *user equilibrium* is reached when no vehicle can lower its transportation cost through unilateral action. It is for instance used in road network applications, where roads do not have infinite capacity but the number of vehicles that can use each road in a given amount of time is limited.

The previously mentioned problems take into account the arcs of the graph to define routes, and possibly capacities on these routes. However, there are also other types of problems in which the grain is coarser: nodes are defined by geographical sectors, and a total capacity on each of these sectors is imposed.

This special case, therefore, involves capacities on the *vertices* of the graph. This type of problem appears in air transportation: it is then named *air traffic flow management problem* (ATFMP), originally defined in [27]. The objective function of the ATFMP is the total cost of aircraft delays, but variants can be derived by considering other objective functions. For example, the total cost of trajectories in terms of flight time, distance flown, or CO_2 emitted can be taken into account. Optimization models addressing this problem typically involve the following decisions to be made for each flight:

- which sector to fly and when (which may induce speed modulations)?
- when to take off (by imposing delays with respect to the scheduled departure time)?

Various capacity upper bounds are imposed on:

- the total number of aircraft in each sector at any given time (sector capacity constraints),
- the total number of aircraft in each airport at any given time (airport capacity constraints).

This is a large-grained problem, but it is also necessary to take into account the more precise spatial scale of the arcs to know where to fly through a sector at a given time. This is done in the variant of the ATFM problem that involves rerouting (*Air Traffic Flow Management with Rerouting Problem*), and is solved in [28] (in its deterministic version). The level of detail in this problem is very high since it completely defines the trajectory followed, and it decides the speed of each aircraft on flown arcs. It takes into account the cost on each arc. This cost can be the flight time, the distance flown, or estimated CO_2 emissions on this arc, for each aircraft. This problem is usually addressed well in advance of takeoffs, several hours to several days before.

This paper proposes a method to organize traffic while ensuring safety by satisfying capacity constraints on sectors. Moreover, it is also able to take into account contrails for minimizing the traffic environmental impact. The methodology proposed allows one to compute trajectories a few hours before takeoffs or to compute them in a quasi-real-time framework, by taking benefit of enriched information as time goes.

3 Mathematical Optimization Model

This section presents the mathematical optimization models for the subgraph-capacity multiple shortest-path problem. Section 3.1 presents the static case. This model is a building block for the time-dependent case, addressed by a heuristic described in Section 3.2.

3.1 Static Case

This subsection focuses on the subgraph-capacity multiple shortest-path problem in the static case (input data do not evolve with time).

The classical shortest-path problem on a graph involves only one vehicle. It is defined on a weighted graph $G = (V, A)$, where V is the set of vertices, A is the set of arcs, and $w : A \to \mathbb{R}$ is the weight function. The model is built with the decision-variable vector X that has component $x_{u,v}$ for each arc $(u, v) \in A$, where $x_{u,v}$ indicates whether the arc (u, v) is part of the solution path or not, minimizing the cost of the solution path and satisfying classical flow constraints (see, for instance, [16]) from the starting node $s \in V$ toward the ending node $e \in V$.

This classical problem can be adapted in the case of several vehicles with vehicle-specific weight functions, whose (u, v, i)-component is noted $w_{u,v,i},\ (u, v) \in A,\ i = 1, 2, \ldots, M$, where M is the number of vehicles, and for each vehicle $i = 1, 2, \ldots, M$, a start vertex $s_i \in V$, and an end vertex $e_i \in V$ are given. The model is built with the decision-variable vectors X_i whose (u, v, i)-component is equal to 1 if the arc (u, v) is part of the solution path for flight i and to 0 otherwise.

Finally, a subgraph-capacity extension can be defined, provided a set cover $\bigcup_{k=0}^{N} A_k = A$ of the set of arcs is given with corresponding capacities $C_k,\ k = 1, 2, \ldots, N$, where N is the number of arc subsets considered. In the sequel, we shall call *sector* each of these arc subsets. This model can also be compared with capacited network flow models [29]. In general, in such models, capacity constraints are defined on arcs [30] or on nodes [31]. In our case, the capacity constraints are defined on subsets of the arc set.

We define an auxiliary decision-variable vector, Y_i, for each vehicle $i,\ i = 1, 2, \ldots, M$, whose (k, i)-component $y_{k,i}$ is equal to 1 if vehicle i uses arcs of sector $A_k,\ k = 1, 2, \ldots, N$ and to 0 otherwise. The optimization model for the subgraph-capacity multiple shortest-path problem is then:

$$\min_{X,Y} \quad \sum_{i=1}^{M} \sum_{(u,v)\in A} w_{u,v,i} x_{u,v,i} \tag{1a}$$

$$\text{s.t.} \quad \sum_{(u,v)\in A} x_{u,v,i} - \sum_{(v,u)\in A} x_{v,u,i} = 0, \quad u \in V \backslash \{s_i, e_i\}, \quad i = 1, 2, \ldots, M \tag{1b}$$

$$\sum_{(s_i,v)\in A} x_{s_i,v,i} - \sum_{(v,s_i)\in A} x_{v,s_i,i} = 1, \quad i = 1, 2, \ldots, M \tag{1c}$$

$$\sum_{(e_i,v)\in A} x_{e_i,v,i} - \sum_{(v,e_i)\in A} x_{v,e_i,i} = -1, \quad i = 1, 2, \ldots, M \tag{1d}$$

$$\sum_{i=1}^{M} y_{k,i} \leq C_k, \quad k = 1, 2, \ldots, N \tag{1e}$$

$$y_{k,i} = 1 \text{ if and only if } \sum_{(u,v)\in A_k} x_{u,v,i} \geq 1, \quad \begin{matrix} i = 1, 2, \ldots, M, \\ k = 1, 2, \ldots, N \end{matrix} \tag{1f}$$

$$\sum_{(u,v)\in A} t_{u,v,i}\, x_{u,v,i} \leq (1 + \eta_i)\, t_{0,i} \quad i = 1, 2, \ldots, M \tag{1g}$$

$$X_i \in \{0, 1\}^{|A|}, \quad i = 1, 2, \ldots, M \tag{1h}$$

$$Y_i \in \{0, 1\}^{N}, \quad i = 1, 2, \ldots, M, \tag{1i}$$

where $\eta_i > 0, i = 1, 2, \ldots, M$, is a user-defined parameter. Constraints (1b), (1c), and (1d) are the usual path flow conservation constraints for each vehicle, and constraints (1e) and (1f) are the new subgraph-capacity constraints. Constraints (1f) enforce the definition of the auxiliary binary variables $Y_1, Y_2, \ldots, Y_M$. These constraints can be linearized and the Y_i's can be relaxed into continuous variables, as shown below by Proposition 1. Constraints (1g) are used to force the travel time ($\sum_{(u,v)\in A} t_{u,v,i}\, x_{u,v,i}$) for each vehicle i to be less than $1+\eta_i$ times a reference travel time. This is an optional constraint that prevents one or more vehicles from being significantly more penalized than others. This can also be desirable when there are constraints on reusing a vehicle for another journey, for example.

Proposition 1 *Each of the constraints* (1f)*, $i = 1, 2, \ldots, M$, $k = 1, 2, \ldots, N$, can be replaced and linearized by:*

$$y_{k,i} \geq x_{u,v,i}, \quad (u, v) \in A_k, \tag{2}$$

$$y_{k,i} \leq \sum_{(u,v)\in A_k} x_{u,v,i}, \tag{3}$$

$$y_{k,i} \in [0, 1]. \tag{4}$$

Proof Consider a sector k and a vehicle i. One can easily show that $1 - y_{k,i} = \prod_{(u,v)\in A_k} (1 - x_{u,v,i})$. Applying then the classical Fortet linearization extended to a product of several binary variables (see [32], Subsection 3.3.2),

$$1 - y_{k,i} \leq 1 - x_{u,v,i}, \quad (u, v) \in A_k,$$

$$1 - y_{k,i} \geq 1 - \sum_{(u,v)\in A_k} x_{u,v,i},$$

$$1 - y_{k,i} \in [0, 1].$$

This yields straightforwardly the desired result.

3.2 Heuristic Approach for the Time-Dependent Case

This subsection defines the mathematical formulation of the problem in the case where input data evolve with time. In the general case, we are considering time-dependent costs. Moreover, constraints (1e) and (1f) are time-dependent in the case where a sector is only occupied by the vehicle during a certain amount of time and it is not occupied when the vehicle is not in the sector yet/anymore. The associated time-discretized model is detailed in Appendix A. This model cannot be used for a quasi-real-time application for two main reasons. First, the computation time required for solving directly the time-discretized model is too high. Some work has focused on pre-processing tasks to overcome this problem, especially in the ATFM problem framework such as in [28, 33]. A low computation time is necessary in a quasi-real-time context but also when addressing the problem a few hours before takeoffs since computations can be done several times, for comparing several scenarios for instance. However, there remains an issue with an approach based on the time-discretized model in the context of this study. Indeed, it is not adapted to the case of recomputation in the event of updated information (costs, aircraft positioning, capacity), since the entire computation has to be performed again with full knowledge of all the information for the entire period under consideration.

To take into account the release of the capacity of sectors by vehicles as they move, the paths are optimized for a succession of *(sliding) time windows*. More precisely, the paths on the graph are computed based on sector occupancy during the time interval under consideration. Then, the time is incremented by the sliding-window length Δt, and the start vertex s_i of each vehicle i is updated: it is replaced by the vertex reached by vehicle i in the previous sliding-window optimization. This process is illustrated by Fig. 1. When, at the end of a time window, a vehicle is on an arc but not at a node,

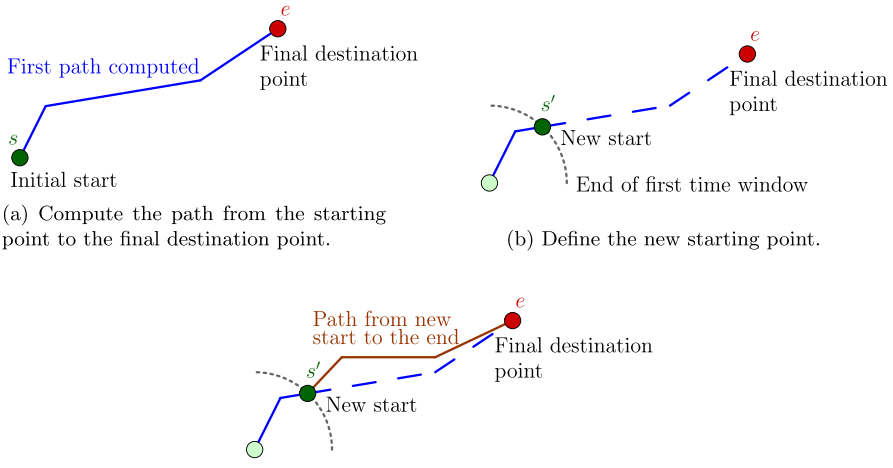

(a) Compute the path from the starting point to the final destination point.

(b) Define the new starting point.

(c) Compute the path from the new starting point to the final destination point.

Fig. 1 Sliding-window computation of a shortest path. The final path is computed sequentially, in pieces, for each of the time windows

an artificial node is created. The process is stopped when each vehicle i has reached its final destination vertex e_i, $i = 1, 2, \ldots, M$. The entry time in the simulation of each vehicle is not artificially changed to coincide with the beginning of a time window. This time-window approach may lead to suboptimal solutions. It is used as a resolution heuristic for the following reasons. First, the time-dependent shortest path for a single vehicle is already a difficult problem [34], not to mention the case involving several vehicles plus capacity constraints. Moreover, in the context of our air transport application, the time-window methodology is tailored to operational concerns. Indeed, all relevant information is not always known for the subsequent time slots, and this time-sequential approach reduces drastically the uncertainties at each time window, by taking into account updated information.

The time-window approach that we are proposing may clearly lead to suboptimal solutions; it is thereby used here as a heuristic but it has several advantages over an approach based on the time-discretized model. First, the time-dependent shortest path for a single vehicle is already a difficult problem [34], not to mention the case involving several vehicles plus capacity constraints. Second, in the case where the computations are done a few hours before takeoffs, it helps to reduce the computation time. Finally, it is particularly adapted to the quasi-real-time framework. Indeed, the time-window approach fixes the information for the duration of the time window, and updates the different costs, capacities, and positions when a new time window is considered.

The paths on the graph are computed taking into account capacity reduction due to a vehicle crossing the sector for a time period longer than the time-window size defined by an *anticipation parameter*, $K \geq 1$, whose precise value is set by the user. This is illustrated by Fig. 2. More precisely, constraints (1f) are modified as follows:

$$y_{k,i} = 1 \text{ if and only if } \sum_{(u,v)\in A_{k,K\,\Delta t}} x_{u,v,i} \geq 1, \quad \begin{matrix} i = 1, 2, \ldots, M, \\ k = 1, 2, \ldots, N, \end{matrix} \tag{5}$$

where $A_{k,K\,\Delta t}$ is the subset of arcs from A_k that have at least one end reachable by vehicle i from s_i within a time less than $K\,\Delta t$. The anticipation parameter, K, allows one to anticipate somehow future time windows. This improves safety in cases where uncertainties may occur in the knowledge of vehicle position and speed. For example, if the vehicle's true position is updated at the end of a sliding window, positioning errors will be mitigated. This is particularly interesting in the case of quasi-online optimization.

4 Application to Contrail Avoidance and CO_2 Minimization

Section 4.1 shows that contrail avoidance for several aircraft can be seen as an instance of the time-dependent subgraph-capacity multiple shortest-path problem modeled in Section 3. Then, the cost-function computation is detailed in Section 4.2. Finally, Section 4.3 details the required input data.

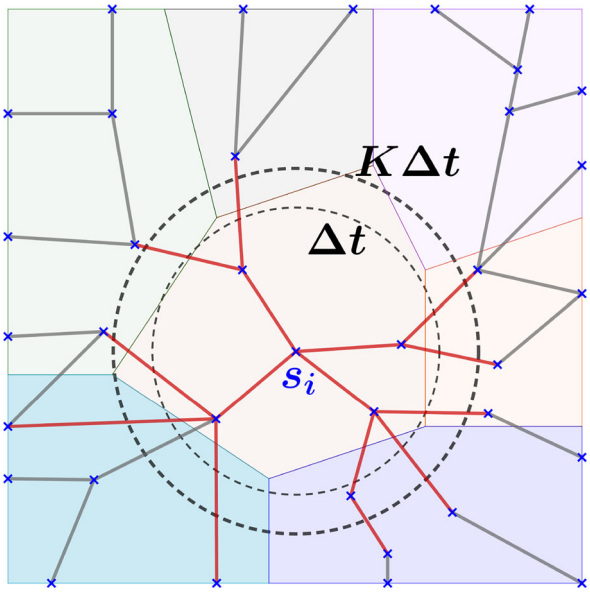

Fig. 2 Capacity computation along time windows. We consider that a vehicle i consumes the capacity of the sectors that are reachable from the start point s_i within a time less than $K\ \Delta t$ (here: capacity is consumed only on red arcs)

4.1 General Description of the Application

In the sequel, the French upper airspace is considered. Aircraft fly above France following a sequence of 3D or 2D points linked by straight-line segment routes. These points are named *waypoints*, and all the waypoints defined above France are the vertices of the graph. The segment routes defined between the waypoints define the set of arcs of the graph. The graph is thereby a directed graph, since aircraft routes are typically constrained to one direction. The problem of finding a trajectory for a flight, therefore, boils down to finding a path in a graph. The aim here is to minimize the global impact of all flights on the environment. More precisely, the goal is to minimize the total environmental cost while ensuring that the airspace capacities are not exceeded. The controller point of view is taken into account, and fairness among aircraft and airlines must be kept in mind. For this reason, and in order to avoid suboptimal solutions, a sequential (one aircraft at a time), greedy-like, computation of trajectories cannot be used, even though there are very efficient algorithms to solve single-vehicle shortest-path problems.

The problem is designed to compute only the *cruise* part of the trajectories. Indeed, departing and arriving an airport is subject to numerous extra operational constraints that leave almost no degree of freedom. Moreover, the altitudes concerned by the contrails are cruising altitudes which are quite high. It is, therefore, generally not relevant to address low-altitude parts of the trajectories. Then, the application we consider in this study is solved only in the 2D plane, i.e., the altitude is not to be decided by the optimizer. The altitude is generally little modified during the cruise phase for reasons of passenger comfort. It is moreover already optimized by airlines

to minimize fuel consumption and reduce engine worn out. Finally, the point of view chosen in this study is that of air traffic control. However, the weight of the aircraft being part of commercial data, it is not known by air traffic control. Without this data, it is not possible to know the ability of the aircraft to climb and to quantify precisely the environmental impact of a climb or a descent.

In the case of ground transportation, applications involving for instance cars on a road network, one can set a limited capacity per arc. In our air transportation application, the capacity limit is on areas (subsets of arcs), called *sectors*. These sectors represent subdivisions of the upper airspace, and more precisely a set cover of the set of arcs. If the trajectories were to be computed sequentially, then some vehicles, the first ones, would be favored over the others. However, in the case of air transport, from the point of view of air traffic control, no airline should be favored over another, so such a sequential approach is not satisfactory. Above all, on the simple point of view of optimization, the greedy-like sequential approach is likely to lead to undesirable, suboptimal solutions.

Remark that satisfying capacity constraints allows one to ensure safety on the strategic time scale (several hours before takeoffs) that is considered here. It guarantees that the controllers will be able to manage the number of aircraft in their sector, while avoiding possible losses of separation in the shorter term.

Airspace capacities evolve with time and their occupancy evolve as aircraft enter or leave airspaces. Moreover, weather data, and also wind and contrail area data, evolve with time. The sliding-window approach is particularly adapted in this case for several reasons. Airspace capacities are defined on given time slots (in number of aircraft per time slot), and can be adapted from a time slot to another. It is also adapted for contrail area consideration since weather predictions are given for a period of time and are refined as time runs. Additionally, this technique can be seen as a quasi-real-time optimization technique. As previously mentioned, weather forecasts are evolving, so it is possible to update them, but it is also possible to update aircraft positions. The speed of planes may occasionally deviate from the reference value, causing them to fly faster or slower. As a result, positions can be updated by implementing a quasi-online optimization strategy, which motivates the use of the anticipation parameter K as illustrated in Fig. 2.

Remark that sectors can, in some cases, be *reconfigured* (sector grouping or splitting) to accommodate demand. In this study, the areas are considered static (the airspace configuration does not evolve with time).

4.2 Cost Computation

As explained before, the goal here is to take into account CO_2 and non-CO_2 effects, and our application focuses on contrails. Then, in the sequel, the only non-CO_2 effect considered will be contrails. Reducing contrails because of their impact aims to avoid favorable areas, or reducing the time (or distance) flown in these areas. Bi-objective optimization is, therefore, a natural point of view to balance the two criteria which may be contradictory (burn more fuel - CO_2 - to avoid contrails - non-CO_2). However, the aim is to minimize the global environmental impact, and for this, we use a metric

that is common in the climate-change literature [15, 35, 36] to balance the two effects. Indeed, it is difficult to make decisions on these parameters independently, when the aim is to minimize the total impact on the environment. The cost, $w_{u,v,i}$ of an arc (u, v) for aircraft i is, therefore, the result of the (weighted) sum of the CO_2 and contrail costs: $w_{u,v,i} = w^{CO_2}_{u,v,i} + w^{\text{contrails}}_{u,v,i}$. As mentioned before, the only non-CO_2 impact considered in this study is the contrail phenomenon: $w^{\text{non-CO}_2}_{u,v,i} = w^{\text{contrails}}_{u,v,i}$. To quantify the relative impact of contrails versus that of CO_2, we use the *Global Warming Potential* (GWP) metric. Since the goal is to minimize the overall impact, it is necessary to quantify the relative impact of contrails versus that of CO_2. For this, a metric known as *Global Warming Potential* (GWP) is used. This metric relates the impact of most greenhouse gases to the impact of CO_2, under the form of a multiplicative factor, considering that the impact of CO_2 corresponds to GWP $= 1$. It acts as a penalty for flying through areas favorable to contrails in a "soft obstacle" approach, considering that all areas produce contrails with the same impact on the climate. This metric depends on a time horizon over which the impact is computed. More details about GWP can be found in [3]. Table 1 gives different values of GWP for contrails according to the different considered time horizons, H. In the sequel, the *contrail-induced cirrus* (CIC) GWP will be noted g_H.

Depending on the time horizon H considered, the contrails have more or less weight. Notably, they have less impact compared to CO_2 in the long term. The parameter H could, therefore, be interpreted as a parameter controlling the respective weight of the two criteria (CO_2 and contrails). In the following, only cirrus clouds induced by contrails will be taken into account, since they are the most impacting effect on the climate. However, other contrails can also easily be considered by our model, by a simple change in the cost function. Then, the cost for an arc (u, v) flown by an aircraft i is: $w_{u,v,i} = (1 + \lambda_{u,v}\, g_H)\, w^{CO_2}_{u,v,i}$, where $\lambda_{u,v} \in [0, 1]$ is the proportion of the arc (u, v) that lies is in a persistent contrail area.

Concerning the cost of CO_2, it is the total quantity of CO_2 emitted by the aircraft as it flies over the arc. The amount of CO_2 emitted per liter of standard jet fuel is constant. This cost is then directly proportional to the fuel consumption. Then, $w^{CO_2}_{u,v,i} = C_{CO_2}\, f_{u,v,i}\, t_{u,v,i}$, where C_{CO_2} is the constant quantity of CO_2 emitted by 1 kg of standard jet fuel, $f_{u,v,i}$ is the fuel flow of aircraft i above the arc (u, v), and $t_{u,v,i}$ its flight time. Then, the cost-function reads:

$$w_{u,v,i} = (1 + \lambda_{u,v}\, g_H)\, C_{CO_2}\, f_{u,v,i}\, t_{u,v,i}. \tag{6}$$

In the case studied, the aircraft evolve in the 2D plane and are assumed not to change speed. The fuel flow is then more or less constant and can be approximated by

Table 1 *Global Warming Potential* for contrail for various time horizons, H

	$H = 20$ years	$H = 100$ Years	$H = 500$ years
$\text{GWP}_{\text{contrail}}(H)$	0.74	0.21	0.064
$\text{GWP}_{\text{CIC}}(H)$	2.2	0.63	0.19

a representative fuel flow (given altitude and speed, representative mass of the cruise phase), f_i^r. Then, the cost function is rather written as:

$$w_{u,v,i} = (1 + \lambda_{u,v}\, g_H)\, f_i^r\, t_{u,v,i}, \tag{7}$$

where multiplicative constants have been removed.

As mentioned earlier, a sliding-window approach is adapted to the case of such weather-dependent cost functions, since there are uncertainties on weather forecast. In particular, contrails are difficult to predict, and their impact is even more difficult to predict [37]. Considering short-term path computation mitigates the uncertainties.

Details about how weather data are processed for the cost-function computation can be found in Appendix B.

4.3 Data

This subsection details the input data of the problem. It explains in particular how the graph is built, and how the sectors are defined. The wind encountered and the areas favorable to contrails are also known data but the process to obtain the related information is detailed in Appendix B.

The present study follows the new principle of *Free Route Airspace* (FRA) which is applied nowadays to the European upper airspace. The aim of FRA is to remove the previously established principle of air routes, and to replace it by navigation points, called waypoints, through which aircraft pass freely. A flight plan is, therefore, a simple sequence of waypoints through which the aircraft flies. This new paradigm allows one to consider an increased number of possible direct routes. As a consequence, the distance flown and thereby the CO_2 emissions, can be decreased.

Rules are still established to fly from a point to another even if their number aims to be decreased. Here, these rules are approximated by the rules established to build the graph $G = (V, A)$ required for the optimization model. The vertex set, V, is the set of considered waypoints. The arcs (set A) connect two waypoints when their inter distance is less than some user-defined threshold distance, $\overline{D}$. One could alternatively consider the complete graph, but this would not be coherent with operational practice, not to mention the increase of complexity in regard with the preliminary nature of the present study.

We construct instances based on the French waypoints that are located in the western and southern parts for now, see Fig. 3 (the arcs are not displayed as they depend upon the maximum threshold distance, $\overline{D}$, chosen).

Our set of arcs is, therefore,

$$A = \{(u, v) \mid u \in V, v \in V, d_{u,v} \leq \overline{D}\}, \tag{8}$$

where V is the set of waypoints, and $d_{u,v}$ is the distance between waypoints u and v.

For the subgraph capacities, the set cover of the set, A, of arcs yields N subsets, called sectors, $\{A_k\}_{k=1,2,\ldots,N}$, initially defined with respect to the waypoint set, as shown in different colors in Fig. 4 for our instances. Then, all arcs with one of its ends

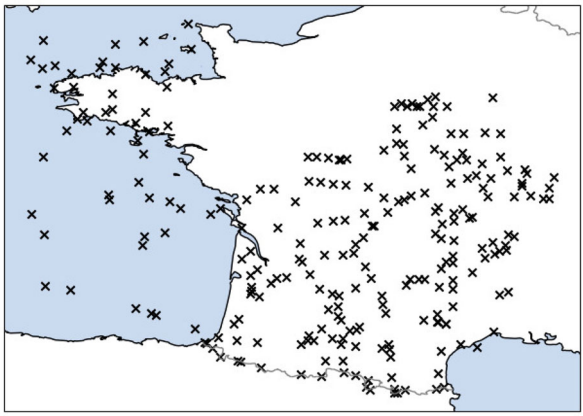

Fig. 3 The FRA waypoints above France constituting our instance set

in one such waypoint set, noted V_k for some $k = 1, 2, \ldots, N$, is considered to be in the (arc-set) sector: $A_k = \{(u, v), u \in V_k \text{ or } v \in V_k\}$.

The next section reports computational results.

5 Results and Sensitivity Analysis

This section presents an illustrative instance of the subgraph-capacity multiple shortest-path problem together with various results obtained from numerical experiments resulting from a sensitivity analysis of the different parameters involved. An example of results is given in Section 5.1. Then, Section 5.2 focuses on the impact of wind on the results, while Section 5.3 addresses the impact of the time horizon chosen

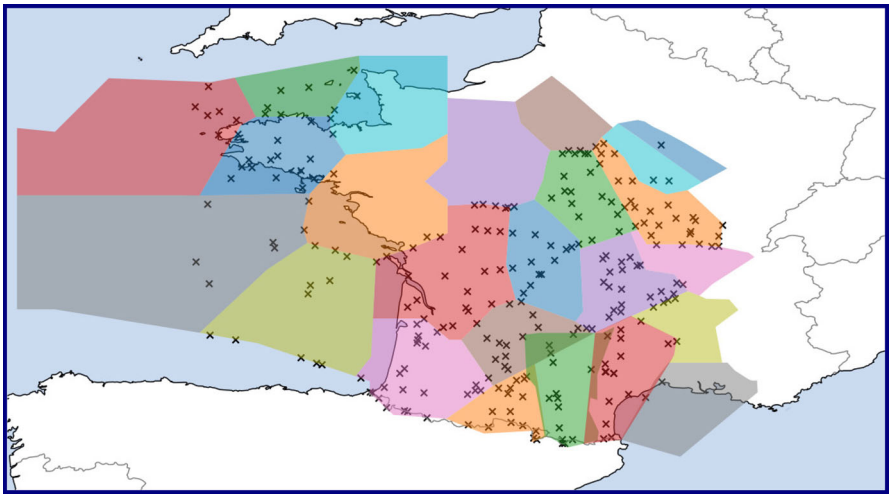

Fig. 4 The vertex subsets V_k's considered above France for building the arc-set sectors A_k's for our instances

for the GWP computation on the results. Finally, the impact of the imposed airspace capacity, C_k, for sector A_k, $k = 1, 2, \ldots, N$, is discussed in Section 5.4.

5.1 Description of the Illustrative Instance

In the sequel, one instance of the problem is addressed but with various cost functions and various levels (right-hand side) for the capacity constraints. This subsection details the definition of this instance.

The graph is computed thanks to rules detailed in Section 4 (see Figs. 3 and 4). Twenty aircraft are entering (taking off or entering the French upper airspace) per 30 min simultaneously, for 3 h. The source-end vertex pair (s_i, e_i) of each aircraft i, $i = 1, 2, \ldots, M$, is chosen randomly in the vertex set so that the minimum distance (as the crow flies) is 200 nautical miles (a Nautical Mile (NM) is the distance unit used in aeronautics, and corresponds to 1.852 km). The resulting instance is named FRA-200. In order to define the arc set, A, we set the maximum distance between two linked points to $\overline{D} = 75$ NM. The airspeed of all aircraft is set to 400 knots (a knot (kt) is the speed unit used in aeronautics and corresponds to 1 NM/h or 1.852 km/h). This speed is chosen in adequacy with the typical airspeed of a standard commercial aircraft, namely the Airbus A320 [38]. Then, to simplify the presentation, the fuel flow is assumed to be the same for all flights (identical aircraft types, engines, and weights). Figure 5 displays the wind encountered, and Fig. 6 shows the persistent contrail areas.

The length of the sliding window for time-dependence consideration is set to $\Delta t = 15$ min. The parameter K for capacity consumption (as defined in Eq. (5)) is set to $K = 1.25$. If nothing else is explicitly mentioned, it is considered that:

- the capacity of each sector k is set to $C_k = 20,\ k = 1, 2, \ldots, N$;
- the time horizon chosen for the GWP computation is set to $H = 100$ years;
- the anticipation parameter K (defined in Eq. (5)) is set to $K = 1.25$;
- the parameter η_i of each flight $i = 1, \ldots, M$ is fixed to an infinite value, i.e., the flight time is not constrained (in other words, constraints (1g) are not considered).

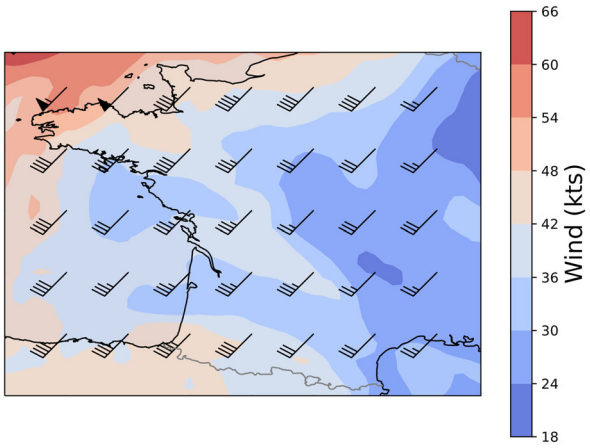

Fig. 5 Wind encountered in instance FRA-200

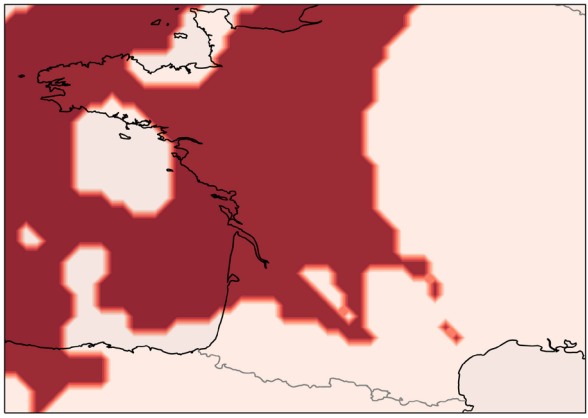

Fig. 6 Persistent-contrail areas used for instance FRA-200

Table 2 summarizes the features of instance FRA-200. More details about the instance can be found in [39].

Instance FRA-200 is solved using the sliding window process explained in Section 3.2. The following results are obtained with the Java API of CPLEX [40] on a computer with an Intel Core i5-10210U, 1.60 Hz, with 8 Go RAM and a Debian Linux OS. The code is available at [41]. Figure 7 shows the solution obtained on instance FRA-200 on maps. The trajectories are represented by groups of 20 aircraft on different maps for reading purposes. The computation time is 137.2 s.

5.2 Impact of Wind

The wind has a certain impact on the results. To quantify this impact, we solve two variants of instance FRA-200:

Table 2 Features of the illustrative instance, FRA-200

Feature	Notation	FRA-200
Aircraft and trajectory features		
Number of aircraft	M	20 per 30 min for 3 h
Airspeed of aircraft		400 kts
Minimum distance between s_i and e_i		200 NM
Airspace features		
Number of sectors	N	23
Maximum distance for arc definition	$\overline{D}$	75 NM
Capacity of each sector	C_k	20
Optimization model features		
Time-window length	Δt	15 min
Time horizon for the GWP computation	H	100 years

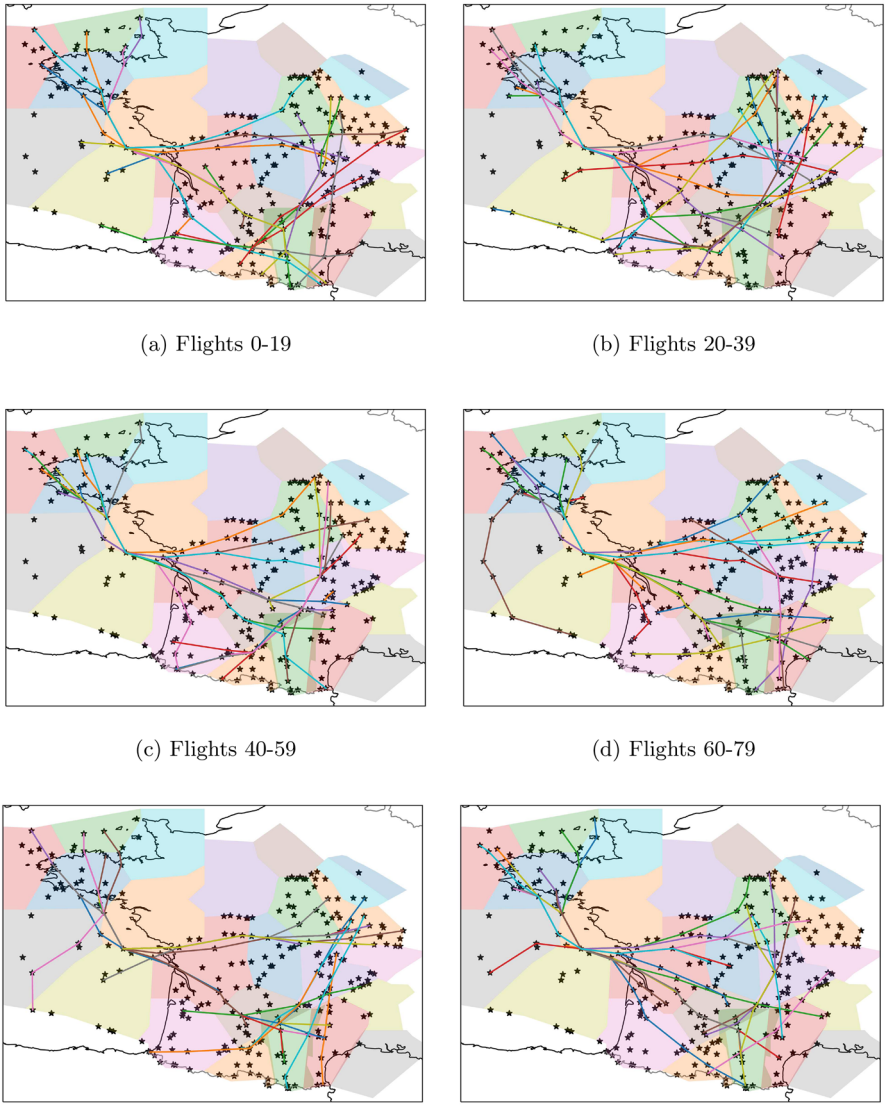

(a) Flights 0-19 (b) Flights 20-39

(c) Flights 40-59 (d) Flights 60-79

(e) Flights 80-99 (f) Flights 100-119

Fig. 7 Results obtained on instance FRA-200, grouped by 20 aircraft, sorted by increasing entry time

1. without wind and without contrails: $w_{u,v,i} = d_{u,v},\ (u,v) \in A,\ i = 1,2,\ldots,M$;
2. with wind and without contrails: $w_{u,v,i} = t_{u,v},\ (u,v) \in A,\ i = 1,2,\ldots,M$.

Figure 8 displays the additional flight distance and flight time in the second case (with wind) in comparison with the first case (without wind).

The results show that in general, the flight distance is increased to the benefit of a reduced flight time, which was expected.

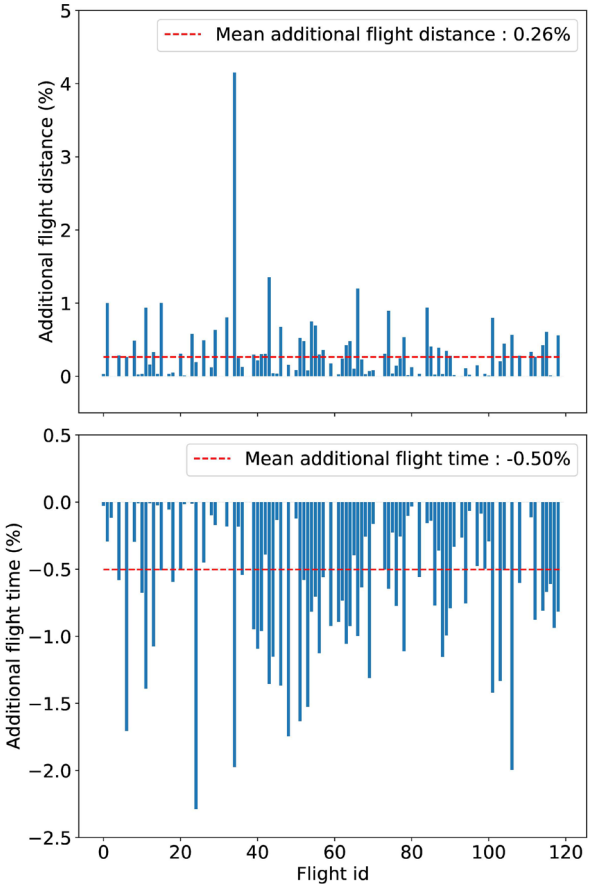

Fig. 8 Additional flight time and flight distance when the wind is considered (flight time minimization) in comparison with results obtained when the wind is not taken into account (only distance is minimized: $w_{u,v,i} = d_{u,v}$)

5.3 Impact of the Time Horizon Used for GWP Computation

As explained in Section 4.2, the cost factor associated with contrails depends on the chosen time horizon, H. Intuitively, the shorter the time horizon is, the more impact the contrails have, and therefore the more beneficial it is to lengthen the trajectories to avoid contrails. To confirm this thought, we solve three variants of instance FRA-200:

1. no contrail consideration: $g_H = 0$;
2. contrail consideration with $H = 100$ years: $g_H = g_{100} = 0.63$;
3. contrail consideration with $H = 20$ years: $g_H = g_{20} = 2.2$.

Figures 9 and 10 display comparative results for variants 1 and 2, and for variants 1 and 3, respectively.

The flight time is higher because of the avoidance of contrail areas. Figures 9 and 10 show that the dependence on the time horizon is important since in the case of a short horizon, the optimal trajectories are much longer than in the case of a longer time horizon. If the contrail impact is considered high, the flight time has a lower impact

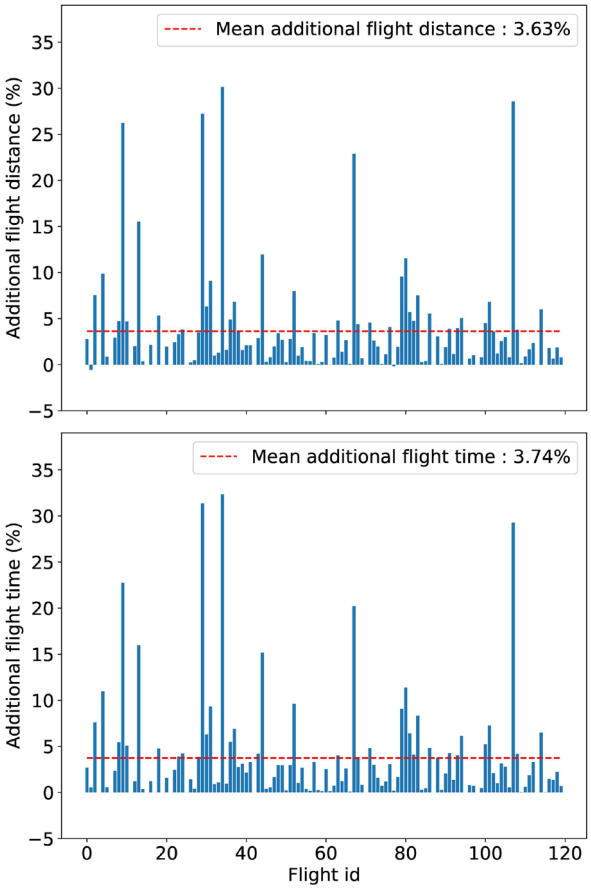

Fig. 9 Additional flight time and flight distance when $H = 100$ years ($g_H = g_{100} = 0.63$) when compared with the case without contrails ($g_H = 0$)

on the objective function, and then is highly increased to avoid as much as possible the areas favorable to contrails. Indeed, Fig. 10 shows optimal trajectories with an increase of more than 30% in flight time. Fuel consumption therefore explodes.

From an environmental point of view, the use of the chosen metric leads to this result. At first sight, this choice seems questionable. Nevertheless, given the assumptions associated with the metric, this result is the one that minimizes the environmental impact, although it may not be operationally acceptable. There are many reasons why this result may not be operationally acceptable. Firstly, some aircraft are clearly at a disadvantage, and it is difficult to know whether they were diverted to avoid contrails, or in order to satisfy capacity constraints. Moreover, the aircraft may have to ensure connections and therefore cannot arrive too late. Finally, the fuel on board must be sufficient not only to make the trip, but also to account for the event of being diverted to another airport, so there is a constraint on the length of the detour. Then, the constraints restricting the detour can be added in the model (through constraints (1g)). Figure 11 shows an example of results obtained when such constraints are added with $\eta_i = 0.1$, $i = 1, 2, \ldots, M$ (10% of additional flight time is allowed).

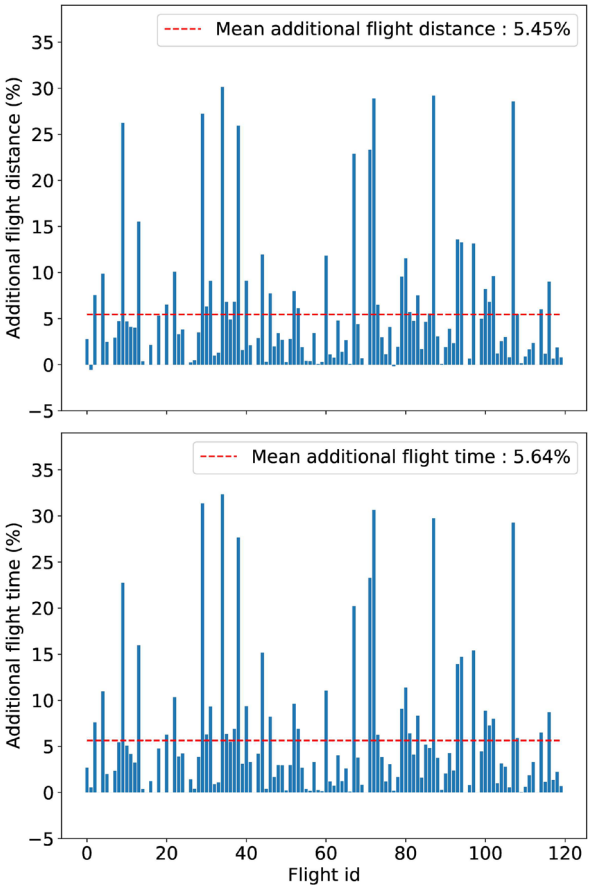

Fig. 10 Additional flight time and flight distance when $H = 20$ years ($g_H = g_{20} = 2.2$) when compared with the case without contrails ($g_H = 0$)

Because of the sliding-window process, the extra constraints are not globally satisfied, but they are satisfied locally at each step, and are nearly satisfied at the global scale, as can be observed in Fig. 11.

5.4 Impact of Airspace Capacity

Another parameter to be studied is each of the airspace capacity values C_k's. The same setup concerning aircraft is taken with a GWP computed with, this time, $H = 100$ years. Several results are impacted by changing the airspace capacity, especially the obtained optimal objective-function value, and the computation time required. Indeed, in order to satisfy capacity constraints, some aircraft may be forced to fly longer or through contrail zones. The problem can be harder to solve if the capacity constraints are too restrictive, and so the computation time increases. Figure 12 shows the evolution of the optimal objective-function value obtained and the computation time required for various capacity levels, C_k, assumed constant for every sector k, $k = 1, 2, \ldots, N$, and at each time window.

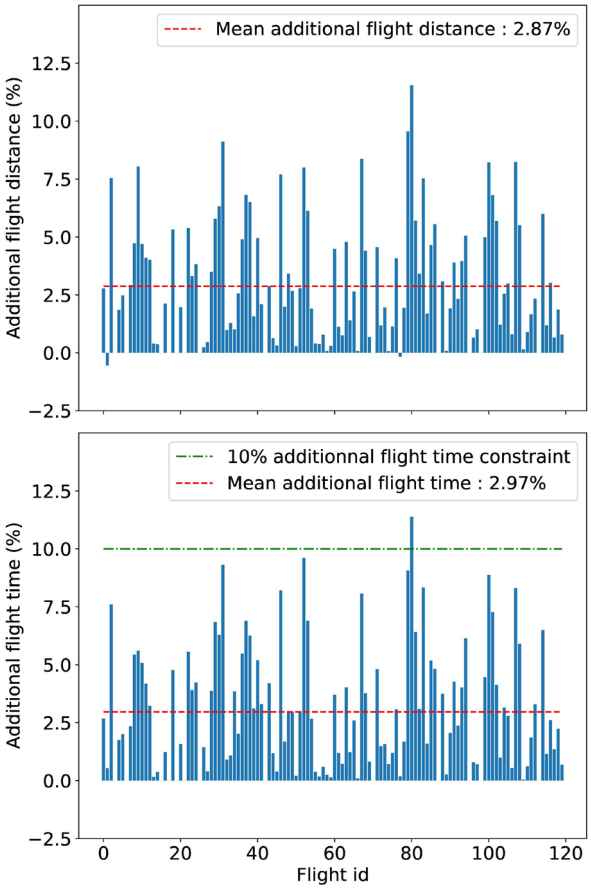

Fig. 11 Additional flight time and flight distance with extra flight time constraints added when $H = 20$ years, in comparison with the case without contrails

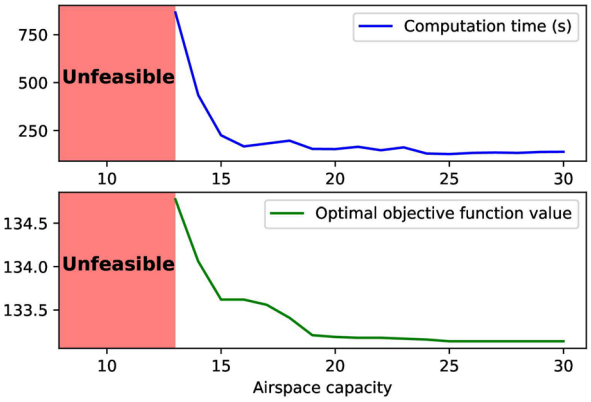

Fig. 12 Result comparison in terms of objective-function value and computation time when the airspace capacity, C_k, changes

The above results show how the right-hand side of the airspace capacity constraints affect the feasibility of the problem and the environmental impact. The higher the capacity of the airspace is, the better the results are. However, beyond a certain value of C_k, no change is observed in computation time, nor in objective-function value since the capacity constraints are not saturated.

5.5 Impact of the Anticipation Parameter

The value of the anticipation parameter K defined in Section 3.2 has an impact on the computation time and on the objective-function value obtained. Solving the illustrative instance FRA-200 for different values of K yields the results displayed on Fig. 13.

One observes that the computation time and the optimal value of the objective function increase with K (rapidly for the computation time). The number of constraints does not increase nor does the number of problems solved, since the size of the time window does not change. However, the capacity constraints (constraints (1e)) become more restrictive, involving more decision variables in the left-hand side term. Figure 14 shows an example considering one aircraft for which the red path is assigned. In this example, if $K = 1.25$, at the current iteration of the algorithm proposed, the aircraft is only counted in sector 1, and not in sector 2. However, if $K = 1.5$, the aircraft consumes capacity in both sectors at the given iteration. The optimization problem is more constrained as the anticipation parameter increases, the optimal value of the objective function can only deteriorate.

The value of the anticipation parameter K should be set according to the use case, depending on the desired level of conservatism in view of increasing safety and robustness to the uncertainty of the position of aircraft (recall however that the value of K should be chosen greater than 1 for the reasons given earlier in Section 3.2). The anticipation parameter allows one to take into account positioning uncertainties in a context of quasi-real time. It also makes it possible to anticipate potential future problems, by reducing the risk of late infeasibility, while avoiding to take into account too far in advance the occupancy of sectors (which would be too restrictive and would make no operational sense). Therefore, the value of K should not be set too high, especially since this would make computing time unreasonably long. The value of this parameter

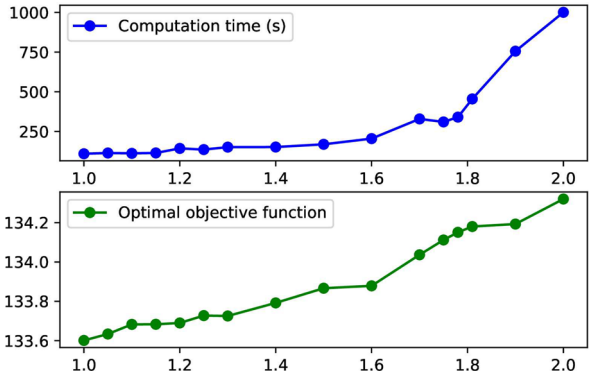

Fig. 13 Result comparison in terms of objective-function value and computation time when the anticipation parameter, K, changes

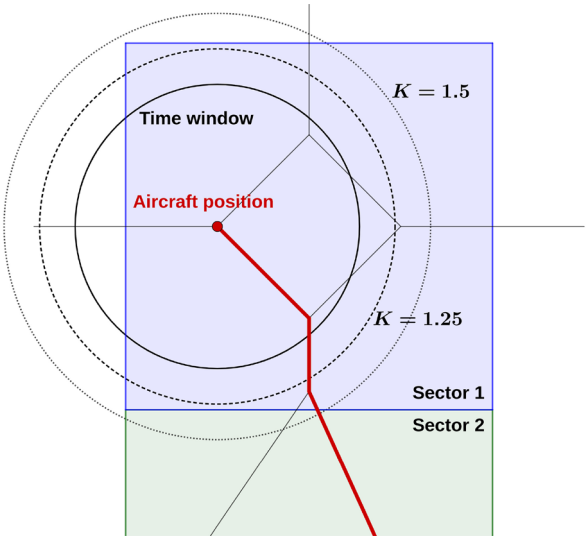

Fig. 14 Example with one aircraft of capacity consumption according to the value of the anticipation parameter K. Here, in the case where $K = 1.25$, the aircraft does not consume any capacity in sector 2, but it does when $K = 1.5$

should be fixed depending on the specific considered application and depending on any computation time limit (e.g., in a quasi-real-time context). For instance, in our computational experiments, the computation time increases drastically when $K > 1.6$. Therefore, if the positioning uncertainties are not too large, a value under 1.6 is clearly desirable.

6 Conclusion

Motivated by the issue of contrail avoidance at the network scale from the air traffic control point of view, we introduced a new model for the multiple shortest-path problem that takes into account capacity constraints on subgraphs. In the static case, the number of vehicles going through each considered subgraph is counted and bounded. Dynamic aspects have also been taken into account by establishing an adapted model with time windows over each of which the static model is solved. Taking this time-dependent aspect into account is essential because as vehicles move, they free up capacity, and costs can also change over time. The model used does not provide the same quality of solution as if the static model had been discretized in time, but it fits better the operational reality as illustrated by the application addressed in our study. Moreover, the proposal methodology allows one to use a standard solver to solve realistic air traffic instances.

The application addressed in this paper motivated the introduction of a new model for the contrail-avoidance problem when considered at the network scale and from the air traffic control point of view. The time-window strategy is particularly adapted to model time-dependency since it can encompass diverse operational features such as time between contrail forecasts and uncertainty on their prediction and airspace capacities defined per time period. The trajectories are computed for all aircraft and

not for each individual aircraft to avoid favoring any particular flight. Work has also been done for computing cost of arcs, so that they can be adapted to the Air Traffic Management point of view. This allows one to consider and to weigh CO_2 and contrail impact using Global Warming Potential with different time horizons, giving more or less importance to contrail avoidance. Moreover, it allows one to take into account other non-CO_2 effects due to air transport, or to use more elaborated metrics to determine the impact of contrails.

Future tracks of research should focus on the numerous sources of uncertainty to be taken into account when addressing the contrail-avoidance problem. There are several uncertainties to consider when studying contrail-favorable (or persistent-contrail-favorable) areas, as shown by Gierens et al. [37]. Other sources of uncertainty are the wind estimation and the presence of traffic.

Furthermore, it is particularly important in air traffic control that one airline is not systematically disadvantaged over another. The simultaneous computation of trajectories helps to limit this pitfall, but fairness consideration is an open area for future research.

Finally, other decision variables could be considered. First, recall that in this study, the airspace configuration is considered static, the sectors are not modified. However, reconfiguration may also be involved in decisions to accommodate the location of contrail areas. Also, the cruise altitude should be envisaged as a decision variable since it is an efficient mean of mitigating contrail impact, as shown by Fichter et al. [42].

This leads to several issues including the knowledge of some critical aircraft parameters (such as its weight at any moment) that are not known from the air traffic control point of view. Moreover, fuel consumption depends on the altitude as well as on the type of aircraft. Models to estimate fuel flows from an air traffic control perspective should be considered. The OpenAP [43] database, or other models based on machine learning, could thereby be used, as in [44] for the approach and landing phases.

Appendix A: Time-Discretized Optimization Model

The mathematical optimization model obtained in the static case can be discretized to obtain the time-dependent optimization model. This transformation is based on the classical *time-dependent shortest-path* problem [45].

Some notations should be defined first:

- $T_i = \{t_{0,i}, \ldots, t_{f,i}\}$: the set of time slots for vehicle i;
- $T = \bigcup_{i=1}^{M} T_i$;
- $C_{k,t}$: the capacity of sector k, $k = 1, 2, \ldots, N$, for time slot t, $t \in T$;
- $w^t_{u,v,i}$: the cost for vehicle i, $i = 1, 2, \ldots, M$, to go through arc $(u, v) \in A$ at time slot t, $t \in T_i$;
- $\Delta^t_{u,v,i}$: the time necessary for vehicle $i, i = 1, 2, \ldots, M$, to go through arc $(u, v) \in A$ at time slot t, $t \in T_i$.

The decision variables are for each vehicle i, $i = 1, 2, \ldots, M$:

- $x_{u,v,i} \in \{0, 1\}$ is equal to 1 if vehicle i goes through arc (u, v);
- $z^t_{u,v,i} \in \{0, 1\}$ is equal to 1 if vehicle i enters arc (u, v) at time slot t;
- $y^t_{k,i} \in \{0, 1\}$ is equal to 1 if vehicle i flies through sector k at time slot t, $t \in T$.

The model is then:

$$\min_{X,Y,Z} \quad \sum_{i=1}^{M} \sum_{t \in T_i} \sum_{(u,v) \in A} w^t_{u,v,i} z^t_{u,v,i} \tag{A1a}$$

$$\text{s.t.} \quad \sum_{(u,v) \in A} x_{u,v,i} - \sum_{(v,u) \in A} x_{v,u,i} = 0,\ u \in V \backslash \{s_i, e_i\},\ i = 1, 2, \ldots, M \tag{A1b}$$

$$\sum_{(s_i,v) \in A} x_{s_i,v,i} - \sum_{(v,s_i) \in A} x_{v,s_i,i} = 1,\ i = 1, 2, \ldots, M \tag{A1c}$$

$$\sum_{(e_i,v) \in A} x_{e_i,v,i} - \sum_{(v,e_i) \in A} x_{v,e_i,i} = -1,\ i = 1, 2, \ldots, M \tag{A1d}$$

$$\sum_{(u,v) \in A} z^t_{u,v,i} - \sum_{(v,u) \in A} z^{t+\Delta^t_{v,u,i}}_{v,u,i} = 0,\ u \in V \backslash \{s_i, e_i\},\ i = 1, 2, \ldots, M,\ t \in T_i \tag{A1e}$$

$$\sum_{(s_i,v) \in A} z^{t_{0,i}}_{s_i,v,i} = 1,\ i = 1, 2, \ldots, M \tag{A1f}$$

$$\sum_{t \in T_i} z^t_{u,v,i} = x_{u,v,i},\ (u, v) \in A,\ k = 1, \ldots, N,\ i = 1, \ldots, M \tag{A1g}$$

$$\sum_{i=1}^{M} y^t_{k,i} \leq C_{k,t},\ k = 1, 2, \ldots, N,\ t \in T \tag{A1h}$$

$$y^t_{k,i} = 1 \text{ if and only if } \sum_{(u,v) \in A_k} z^t_{u,v,i} \geq 1,\ i = 1, 2, \ldots, M,\ k = 1, 2, \ldots, N,\ t \in T_i \tag{A1i}$$

$$y^t_{k,i} = 0,\ i = 1, 2, \ldots, M,\ k = 1, 2, \ldots, N,\ t \in T \backslash T_i \tag{A1j}$$

$$X_i \in \{0, 1\}^{|A|},\ i = 1, 2, \ldots, M \tag{A1k}$$

$$Z_{i,t} \in \{0, 1\}^{|A|},\ i = 1, 2, \ldots, M,\ t \in T_i \tag{A1l}$$

$$Y_{i,t} \in \{0, 1\}^{N},\ i = 1, 2, \ldots, M,\ t \in T_i. \tag{A1m}$$

Constraints (A1b), (A1c), and (A1d) are the flow conservation constraints. Constraints (A1e) and (A1f) enforce consistency of space-time flow conservation. Constraints (A1g) make the link between the time-dependent and the static decision variables. Constraints (A1h) are the time-discretized capacity constraints. Constraints (A1i) and (A1j) define the auxiliary variables $y^t_{k,i}$. The former can easily be linearized, as for the static model using Proposition 1.

A.1 Comparison with the Proposed Heuristic

The resolution of this model via CPLEX [40] has been compared to the proposed heuristic approach. Table 3 shows the different results, with various instance sizes, and two capacity scenarios: one retricting and the other non-restricting, with a time-discretization step equal to the size of the sliding window. In this case, the time window

Table 3 Comparison of the results obtained by solving directly the time-discretized model and using the sliding window approach for three instance sizes and two capacity scenarios

Instance size	Capacity scenario	Method	Computation time	Objective function value
10	Non-restricting	Time-discretized method	95.49 s	8.9828
		Sliding-window approach - $K = 1.25$	11.56 s (-88%)	8.9828 (+0%)
		Sliding-window approach - $K = 1.5$	10.71 s (-89%)	8.9828 (+0%)
	Restricting	Time-discretized method	412.67 s	8.983
		Sliding-window approach - $K = 1.25$	14.02 s (-97%)	8.9948 (+0.13%)
		Sliding-window approach - $K = 1.5$	12.66 s (-97%)	9.0201 (+0.41%)
20	Non-restricting	Time-discretized method	357 s	17.9535
		Sliding-window approach - $K = 1.1$	19.61 s (-94%)	17.9535 (+0%)
		Sliding-window approach - $K = 1.25$	19.72 s (-94%)	17.9535 (+0%)
		Sliding-window approach - $K = 1.5$	20.05 s (-94%)	17.9535 (+0%)
	Restricting	Time-discretized method	613,15 s	17.9657
		Sliding-window approach - $K = 1.1$	21.26 s (-97%)	17.9658 (+0.0005%)
		Sliding-window approach - $K = 1.25$	21.43 s (-97%)	17.9897 (+0.13%)
		Sliding-window approach - $K = 1.5$	22.54 s (-97%)	18.0376 (+0.40%)
60	Non-restricting	Time-discretized method	501.36 s	53.8969
		Sliding-window approach - $K = 1.25$	90.51 s (-82%)	53.8969 (+0%)
		Sliding-window approach - $K = 1.5$	92.44 s (-82%)	53.8969 (+0%)
	Restricting	Time-discretized method	2466 s	53.8976
		Sliding-window approach - $K = 1.25$	95.06 s (-96%)	53.9903 (+0.17%)
		Sliding-window approach - $K = 1.5$	96.26 s (-96%)	54.0925 (+0.36%)

is small, because the discretization step must be smaller than the flight time on the shortest arc. The impact of the value of the parameter K is also studied. These results are presented in Table 3.

One observes differences between the two methods in terms of computation time and objective function value. On the one hand, the heuristic approach yields significantly lower computational times than that obtained by directly solving the time-discretized model. On the other hand, despite differences in the objective function value results, the values obtained with the heuristic approach remain close to those obtained with the exact method. The gain in computation time is what interests us here with regard to the application case. Thus, the loss in objective function is reasonable compared to the computational gain. All the more so as the chosen heuristic enables us to directly take into account the data update at each time interval, whereas solving the discretized model directly requires us to completely redo the computations each time. This low computation time is required when solving the problem in quasi-real-time framework but also a few hours before because computations can be repeated several times, to compare several scenarios for example, and it is essential that computation time is not too long.

Appendix B: Data Processing for Numerical Experiments

This section shows how data for computational experiments have been extracted and computed. Appendix B.1 deals with wind data, while Appendix B.2 focuses on contrail data.

B.1 Wind Data

The costs defined by (7) involve the computation of the flight time over each arc $(u, v) \in A$. To compute these costs, the wind on the arcs, and the distance between u and v, the two ends of the arcs, have to be known.

Let λ_u and λ_v be the latitude of vertices u and v respectively, and let ϕ_u and ϕ_v be their longitude. The distance between u and v is given by:

$$d_{u,v} = R\, c_{rad} \quad \text{in km}, \tag{B1}$$

$$= 60\, c_{degrees} \quad \text{in NM}, \tag{B2}$$

where $R = 6,371$ km is the Earth radius, c_{rad} and $c_{degrees}$ represent the following c values, expressed in radians and in degrees respectively:

$$c = \arccos\Big(\sin(\lambda_u)\,\sin(\lambda_v) + \cos(\lambda_u)\,\cos(\lambda_v)\,\cos(\phi_v - \phi_u)\Big). \tag{B3}$$

Then, the flight time for aircraft i, noted $t_{u,v,i}$, between points u and v is given by:

$$t_{u,v,i} = \frac{d_{u,v}}{GS_{u,v,i}}, \tag{B4}$$

where $GS_{u,v,i}$ is the ground speed of aircraft i on arc (u, v). It can be computed via:

$$GS_{u,v,i} = V_{a_i} + W_{u,v}, \tag{B5}$$

where V_{a_i} is the airspeed of aircraft i (considered constant), and $W_{u,v}$ is the wind encountered on the arc (u, v).

Wind data have been extracted from the website Windy [46] on a square grid of size 0.2° above France, as shown in Fig. 15.

To compute the wind on each node of the graph, a so-called Shepard interpolation [47] was used. More precisely, for each node P located in a 2D-square $P_1P_2P_3P_4$

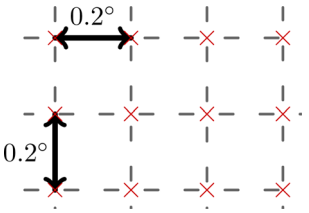

Fig. 15 2D grid used for wind data extraction from Windy [46]

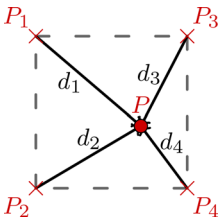

Fig. 16 Notations for estimating the wind at P via Shepard interpolation

of the data grid (see Fig. 16), the wind $W(P)$ at P is calculated from the wind at P_k, $k = 1, 2, 3, 4$, using the distance from P to each of these points (noted respectively d_1, d_2, d_3 and d_4) as follows:

$$W(P) = \frac{\sum_{i=1}^{4} W(P_i) * d_i^{-p}}{\sum_{i=1}^{4} d_i^{-p}}, \tag{B6}$$

where $p > 1$ is a user-defined parameter (set to $p = 2$ in this study).

Finally, the wind along an arc (u, v) is simply defined as the average of that at u and at v:

$$W_{(u,v)} = \frac{W(u) + W(v)}{2}. \tag{B7}$$

Figure 17 shows data used for the examples presented in the result section (Section 5).

B.2 Contrail Data

Contrails are formed in cold and humid areas. They persist and induce cirrus if the air is supersaturated in ice. The computation of persistent contrail areas is performed in two phases:

1. Areas favorable to contrail formation
2. Areas in which contrails will persist (ice supersaturated areas).

In [36], contrail areas are computed thanks to the *Schmidt-Appleman criterion*. This criterion gives a minimum threshold, r_{min}, of relative humidity of the air in liquid water, noted RH_w, above which contrails are formed: contrails are assumed to

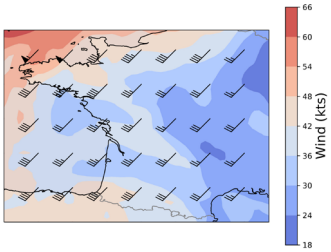

Fig. 17 Wind encountered in the example of the result

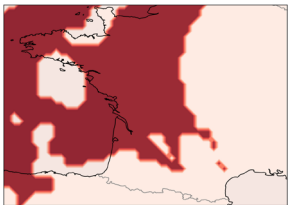

Fig. 18 Persistent-contrail areas in western France used for our instances

form when $RH_w \geq r_{min}$, where

$$r_{min} = \frac{G(T - T_c) + e_{sat}^{liq}(T_c)}{e_{sat}^{liq}(T)}, \tag{B8}$$

$e_{sat}^{liq}(T)$ is the saturation vapor pressure over water, and T_c is the estimated threshold temperature (in Celsius degrees) for contrail formation at liquid saturation. The latter is computed via:

$$T_c = -46.46 + 9.43\log(G - 0.053) + 0.72\log^2(G - 0.053), \tag{B9}$$

where $G = \frac{EI_{H_2O}C_pP}{\epsilon Q(1-\eta)}$, $EI_{H_2O} = 1.25$ is the water vapor emission index, $C_p = 1004\, J.kg^{-1}.K^{-1}$ is the heat capacity of the air, P is the ambient pressure (in Pascals), $\epsilon = 0.6222$ is the ratio of the molecular masses of water and dry air, $Q = 43 * 10^6 J.kg^{-1}$ is the specific heat of combustion, and $\eta = 0.3$ is the average propulsion efficiency of a commercial aircraft.

In [36], the ice super saturated areas are determined thanks to the following criterion: $RH_i > 1$, where the relative humidity over the ice, noted RH_i is computed as follows:

$$RH_i = RH_w * \frac{6.0612 * \exp(\frac{18.102*T}{249.52+T})}{6.1162 * \exp(\frac{22.577*T}{273.78+T})}, \tag{B10}$$

and where T is the ambient temperature in Celsius degrees.

The relative humidity and temperature are also computed from data extracted from Windy [46] on a 2D-grid, and interpolated via quadratic interpolation. Figure 18 shows the data used for the examples presented in the result section (Section 5), where red areas are persistent-contrail-favorable areas, to be avoided.

Acknowledgements The authors thank DGAC (French civil aviation authority) for prompting and funding this work, and more specifically its DTA and DSNA services. Their inputs and expertise were also essential to the achievement of this work. The authors would like to thank Dr. Gabriel Jarry from Eurocontrol for the valuable discussions that contributed to this study.We thank the anonymous reviewers for their valuable remarks which have greatly improved the clarity and the content of this article.

Author Contribution CD: methodology, software, validation, formal analysis, writing. MM: methodology, validation, formal analysis, writing. NC: methodology, validation, formal analysis, writing. DD: methodology, validation, formal analysis, writing. All authors reviewed the manuscript.

Funding The PhD research work of Céline Demouge is funded by DGAC (the French civil aviation authority).

Data Availibility Statement Sample data are available at: https://cloud.recherche.enac.fr/index.php/s/i6jxDFM8GnSAgyF.

Code Availability Code is available in the following reference: [41].

Declarations

Ethical Approval Not applicable

Consent to Participate Not applicable

Consent for Publication Not applicable

Conflict of Interest The authors declare no competing interests.

References

1. Kärcher, B.: Formation and radiative forcing of contrail cirrus. Nature Communications **9**(1), 1824 (2018)
2. Lee, D.S., Fahey, D.W., Skowron, A., Allen, M.R., Burkhardt, U., Chen, Q., Doherty, S.J., Freeman, S., Forster, P.M., Fuglestvedt, J., Gettelman, A., De León, R.R., Lim, L.L., Lund, M.T., Millar, R.J., Owen, B., Penner, J.E., Pitari, G., Prather, M.J., Sausen, R., Wilcox, L.J.: The contribution of global aviation to anthropogenic climate forcing for 2000 to 2018. Atmospheric Environment **244**, 117834 (2021)
3. Fuglestvedt, J.S., Shine, K.P., Berntsen, T., Cook, J., Lee, D.S., Stenke, A., Skeie, R.B., Velders, G.J.M., Waitz, I.A.: Transport impacts on atmosphere and climate: metrics. Atmospheric Environment **44**(37), 4648–4677 (2010)
4. Girardet, B., Lapasset, L., Delahaye, D., Rabut, C.: Wind-optimal path planning: application to aircraft trajectories. In: 2014 13th International Conference on Control Automation Robotics & Vision (ICARCV), pp. 1403–1408 (2014). IEEE
5. Ng, H.K., Sridhar, B., Grabbe, S.: Optimizing aircraft trajectories with multiple cruise altitudes in the presence of winds. Journal of Aerospace Information Systems **11**(1), 35–47 (2014)
6. Legrand, K., Puechmorel, S., Delahaye, D., Zhu, Y.: Robust aircraft optimal trajectory in the presence of wind. IEEE Aerospace and Electronic Systems Magazine **33**(11), 30–38 (2018)
7. Ng, H.K., Sridhar, B., Grabbe, S., Chen, N.: Cross-polar aircraft trajectory optimization and the potential climate impact. In: 2011 IEEE/AIAA 30th Digital Avionics Systems Conference, pp. 3–413415 (2011)
8. Hartjes, S., Hendriks, T., Visser, D.: Contrail mitigation through 3D aircraft trajectory optimization. In: 16th AIAA Aviation Technology, Integration, and Operations Conference. American Institute of Aeronautics and Astronautics, Washington, D.C. (2016)
9. Matthes, S., Grewe, V., Dahlmann, K., Frömming, C., Irvine, E., Lim, L., Linke, F., Lührs, B., Owen, B., Shine, K., Stromatas, S., Yamashita, H., Yin, F.: A concept for multi-criteria environmental assessment of aircraft trajectories. Aerospace **4**(3), 42 (2017)
10. Yin, F., Grewe, V., Frömming, C., Yamashita, H.: Impact on flight trajectory characteristics when avoiding the formation of persistent contrails for transatlantic flights. Transportation Research Part D: Transport and Environment **65**, 466–484 (2018)
11. Rosenow, J., Fricke, H.: Impact of multi-criteria optimized trajectories on European airline efficiency, safety and airspace demand. Journal of Air Transport Management **78**, 133–143 (2019)
12. Campbell, S.E.: Multiscale path optimization for the reduced environmental impact of air transportation. IEEE Transactions on Intelligent Transportation Systems **13**(3), 1327–1337 (2012)

13. Campbell, S., Neogi, N., Bragg, M.: An operational strategy for persistent contrail mitigation. In: 9th AIAA Aviation Technology, Integration, and Operations Conference (ATIO). American Institute of Aeronautics and Astronautics, Hilton Head, South Carolina (2009)
14. Campbell, S., Neogi, N., Bragg, M.: An optimal strategy for persistent contrail avoidance. In: AIAA Guidance, Navigation and Control Conference And Exhibit. American Institute of Aeronautics and Astronautics, Honolulu, Hawaii (2008)
15. Simorgh, A., Soler, M., González-Arribas, D., Matthes, S., Grewe, V., Dietmüller, S., Baumann, S., Yamashita, H., Yin, F., Castino, F., Linke, F., Lührs, B., Meuser, M.M.: A comprehensive survey on climate optimal aircraft trajectory planning. Aerospace **9**(3), 146 (2022)
16. Papadimitriou, C.H., Steiglitz, K.: Combinatorial optimization: algorithms and complexity. Dover Publications, Mineola, N.Y (1998)
17. Dijkstra, E.W.: A note on two problems in connexion with graphs. Numerische Mathematik **1**(1), 269–271 (1959)
18. Hart, P., Nilsson, N., Raphael, B.: A formal basis for the heuristic determination of minimum cost paths. IEEE Transactions on Systems Science and Cybernetics **4**(2), 100–107 (1968)
19. Bellman, R.: On a routing problem. Quarterly of Applied Mathematics **16**(1), 87–90 (1958)
20. Luenberger, D.G.: Introduction to dynamic systems: theory, models, and applications. Wiley, New York (1979)
21. Lozano, L., Medaglia, A.L.: On an exact method for the constrained shortest path problem. Computers & Operations Research **40**(1), 378–384 (2013)
22. Pugliese, L.D.P., Guerriero, F.: A survey of resource constrained shortest path problems: exact solution approaches. Networks **62**(3), 183–200 (2013)
23. Santos, L., Coutinho-Rodrigues, J., Current, J.R.: An improved solution algorithm for the constrained shortest path problem. Transportation Research Part B: Methodological **41**(7), 756–771 (2007)
24. Huang, W., Ding, L.: The shortest path problem on a fuzzy time-dependent network. IEEE Transactions on Communications **60**(11), 3376–3385 (2012)
25. Wardrop, J.G., Whitehead, J.I.: Correspondance. Some theorical aspects of road traffic research. Proceedings of the Institution of Civil Engineers **1**(5), 767–768 (1952)
26. Wardrop, J.G.: Road paper. Some theorical aspects of road traffic research. Proceedings of the Institution of Civil Engineers **1**(3), 325–362 (1952)
27. Bertsimas, D., Patterson, S.S.: The air traffic flow management problem with enroute capacities. Operations Research **46**(3), 406–422 (1998)
28. Agustin, A., Alonso-Ayuso, A., Escudero, L.F., Pizarro, C.: On air traffic flow management with rerouting. Part I: Deterministic case. European Journal of Operational Research **219**(1), 156–166 (2012)
29. Aronson, J.E.: A survey of dynamic network flows. Annals of Operations Research **20**(1), 1–66 (1989)
30. Assad, A.A.: Multicommodity network flows-a survey. Networks **8**(1), 37–91 (1978)
31. Wollmer, R.D.: Maximizing flow through a network with node and arc capacities. Transportation Science **2**(3), 213–232 (1968)
32. Liberti, L.: Reformulation techniques in mathematical programming. HDR thesis (Habilitation à Diriger des Recherches), Université Paris IX, France (2007) https://hal.science/hal-00163563
33. Dal Sasso, V., Djeumou Fomeni, F., Lulli, G., Zografos, K.G.: Incorporating stakeholders' priorities and preferences in 4D trajectory optimization. Transportation Research Part B: Methodological **117**, 594–609 (2018)
34. Foschini, L., Hershberger, J., Suri, S.: On the complexity of time-dependent shortest paths. In: Proceedings of the Twenty-second Annual ACM-SIAM Symposium on Discrete Algorithms, pp. 327–341 (2011). SIAM
35. Sridhar, B., Ng, H.K., Chen, N.Y.: Aircraft trajectory optimization and contrails avoidance in the presence of winds. Journal of Guidance, Control, and Dynamics **34**(5), 1577–1584 (2011)
36. Soler, M., Zou, B., Hansen, M.: Flight trajectory design in the presence of contrails: application of a multiphase mixed-integer optimal control approach. Transportation Research Part C: Emerging Technologies **48**, 172–194 (2014)
37. Gierens, K., Matthes, S., Rohs, S.: How well can persistent contrails be predicted? Aerospace **7**(12), 169 (2020)
38. Airbus A-320 | SKYbrary aviation safety. https://www.skybrary.aero/aircraft/a320
39. Demouge, C.: FRA-200 Instance for subgraph-capacity multiple shortest path application to contrail avoidance (2022). https://cloud.recherche.enac.fr/index.php/s/i6jxDFM8GnSAgyF

40. IBM: ILOG CPLEX optimization studio (2021)
41. Demouge, C., Mongeau, M., Couellan, N.: Time dependent contrails avoidance at network scale. SWHID: <swh:1:dir:b6960b516ab5b62ba6ca4f4037901a3793dcd64c> (2023). https://enac.hal.science/hal-04532626
42. Fichter, C., Marquart, S., Sausen, R., Lee, D.S.: The impact of cruise altitude on contrails and related radiative forcing. Meteorologische Zeitschrift **14**(4), 563–572 (2005)
43. Sun, J., Hoekstra, J.M., Ellerbroek, J.: OpenAP: an open-source aircraft performance model for air transportation studies and simulations. Aerospace **7**(8), 104 (2020)
44. Jarry, G., Delahaye, D., Féron, E.: Approach and landing aircraft on-board parameters estimation with LSTM networks. In: AIDA-AT 2020, 1st Conference on Artificial Intelligence and Data Analytics in Air Transportation, Singapore (2020)
45. Yang, L., Zhou, X.: Constraint reformulation and a Lagrangian relaxation-based solution algorithm for a least expected time path problem. Transportation Research Part B: Methodological **59**, 22–44 (2014)
46. Windyty SE: Windy API. https://api.windy.com/
47. Shepard, D.: A two-dimensional interpolation function for irregularly-spaced data. In: Proceedings of the 23rd ACM National Conference, pp. 517–524. ACM Press, New York (1968)